4-7-2001

A Comparative Analysis of Studies on Heat Transfer and Fluid Flow in Microchannels

Choondal B. Sobhan
Purdue University

Suresh V. Garimella
Purdue University - Main Campus, sureshg@purdue.edu

A Comparative Analysis of Studies on
Heat Transfer and Fluid Flow in Microchannels[1]

Choondal B. Sobhan and Suresh V. Garimella[2]
School of Mechanical Engineering
Purdue University
West Lafayette, Indiana 47907-1288   USA

Tel: (765) 494-5621;   Fax: (765) 494-0539
sureshg@ecn.purdue.edu

ABSTRACT

The extremely high rates of heat transfer obtained by employing microchannels makes them an attractive alternative to conventional methods of heat dissipation, especially in applications related to the cooling of microelectronics. A compilation and analysis of the results from investigations on fluid flow and heat transfer in micro- and mini-channels and microtubes in the literature is presented in this review, with a special emphasis on quantitative experimental results and theoretical predictions. Anomalies and deviations from the behavior expected for conventional channels, both in terms of the frictional and heat transfer characteristics, are discussed.

Amongst the novel methods for thermal management of the high heat fluxes found in microelectronic devices, microchannels are the most effective at heat removal. The possibility of integrating microchannels directly into the heat-generating substrates makes them particularly attractive, since thermal contact resistances may be avoided. The two important objectives in electronics cooling – minimization of the maximum substrate temperature and reduction of substrate temperature gradients – can be achieved by the use of microchannels.

A large number of recent investigations have undertaken to study the fundamentals of microchannel flow, as well as to compare the flow and heat transfer characteristics of microchannels with conventional channels. A comprehensive review of these investigations conducted over the past decade is presented here in concise tabular form.

Predictive correlations have also been proposed in the literature, based on experimental investigations on liquid and gas flow in microchannels. Various combinations of channel size, pitch and substrate material have been considered. Generally, these correlations have been cast in the same forms as conventional relationships for larger-diameter tubes and channels, but have included modified coefficients. A comparative study of the correlations for single-phase flow is presented in this review.

REVIEW OF THE LITERATURE

Studies on microchannel flows in the past decade are categorized into various topics and summarized in Table 1. The literature survey extends over a wide range of topics such as measurement and estimation of friction factor and heat transfer in microchannels and small-diameter tubes, comparison with flow in conventional channels, investigation of single-phase, boiling and two-phase flows in microchannels, mini channels and small tubes, gas flow in microchannels, analytical studies on microchannel flows, and design and testing of microchannel

heat sinks for electronics cooling. For each study, key descriptors of the cooling configuration and the primary observations are included.

QUANTITATIVE COMPARISONS

A comparative study of correlations for single-phase flow and heat transfer in microchannels proposed by various investigators is presented in this section. Correlations for friction factor and heat transfer, in the laminar and turbulent regimes are compared, and contrasted with conventional correlations for macrotubes and channels. Details of each of the studies discussed in this section are available in Table 1.

Friction Correlations

Correlations for friction factor have been proposed based on experiments with nitrogen and water as working fluids [3, 9, 36] in trapezoidal and rectangular channels and microtubes. Peng et al. [13] analyzed water flow in rectangular channels to obtain correlations for various combinations of the channel hydraulic diameter and channel pitch in rectangular channels for laminar and turbulent flow. A plot of the friction factor correlations proposed for laminar and turbulent flow in microchannels is shown in Fig. 1. The graph shows the product of friction factor and Reynolds number (f·Re) plotted against the Reynolds number. Conventional correlations are also included for comparison: the Blasius correlation ($f = 0.140 \, Re^{-0.182}$) is used for turbulent flow, while for laminar flow, circular-pipe ($f = 64/Re$) and square-channel predictions ($f = 57/Re$) are shown. The f·Re product is independent of Reynolds number for laminar flow in conventional channels. In the turbulent regime, the friction factor is almost independent of the Reynolds number (f·Re increases linearly with Re). The predictions in the

literature for microchannels may be analyzed with greater ease by considering the laminar and turbulent regions separately.

Predictions of f·Re in the laminar regime are shown in Fig. 2. The correlations of Wu and Little [3], Choi et al. [9] and Yu et al. [36] predict constant values of f·Re, with the magnitude of this product being greater than for conventional channels in Wu and Little (110), and lower in Choi et al. and Yu et al. (55 and 50 respectively). Predictions from Peng et al. [13] for water flow in rectangular microchannels (see Table 2 for details) show an altogether different trend: in all cases, f·Re decreases with an increase in the Reynolds number. For cases A, B, and C from Peng et al. (in which $D_h \geq 267$ μm), the laminar regime extends to Re ≈ 700, whereas for cases E, F, and G ($D_h \leq 200$ μm), the onset of turbulence occurs as early as Re = 300. (As in the original work, the laminar plots for cases A through D are extended till Re = 1000). While the slopes of the curves for all test cases are identical ($Re^{-0.98}$), the magnitude of f·Re is highest for the largest microchannels (D_h) and lowest for the smallest.

The friction correlations in the turbulent regime are compared with conventional correlations in Fig. 3. Predictions for nitrogen flow from Choi et al. agree very well with conventional results; the Wu and Little correlation is similar to these two in its trend of variation, but the predicted values are much higher in magnitude. The correlations of Peng et al. [13] for water flow again exhibit a very different trend: in all cases, f·Re decreases with an increase in Reynolds number (as $Re^{-0.72}$), in contradiction to conventional correlations. The onset of turbulence is also seen to occur much earlier for the microchannels studied by Peng et al. Another observation of interest in Fig. 3 is that the f·Re values predicted by Peng et al. decrease in magnitude as the channel hydraulic diameter decreases; the drop in f·Re with D_h is very steep when D_h becomes smaller than 200 μm.

Heat Transfer Correlations

Correlations for the average Nusselt number in microchannels in terms of the Reynolds and Prandtl numbers have been proposed in the literature for laminar and turbulent regimes, based on experiments with a range of fluid-substrate combinations, channel dimensions and configurations, as summarized in Table 1.

Heat transfer correlations for nitrogen flow [4, 9, 36], water flow in rectangular microchannels [12, 14, 16], water flow in circular microchannels [20, 36], and methanol in rectangular channels [12] are considered for comparison. Figure 4 shows a composite plot of predicted values of $Nu/Pr^{0.33}$ as a function of Reynolds number from the correlations in these studies. Conventional-channel correlations are also included for comparison: the Dittus-Boelter correlation for turbulent flow in conventional channels, and for laminar flow, $Nu_{Dh} = 1.86 \, (Re_{Dh} \, Pr)^{0.33} \, (D_h/L)^{0.33}$; a sample set of parameters (L = 50 mm and D_h = 0.24 mm) is used to compute values from this correlation. A significant amount of scatter is seen in these plots, as was true for predictions of friction factor, with the predictions of Choi et al. [9] and Yu et al. [36] being among the highest in the turbulent regime. All predictions reflect an increase in Nusselt number with increasing Re.

The heat transfer correlations are again considered separately in the laminar and turbulent regimes in Figs. 5 and 6 respectively. The end of the laminar regime was identified to be at quite different Reynolds numbers in the studies considered, as noted with the friction factor predictions. The dependence of Nusselt number on Reynolds number is stronger in all the microchannel predictions when compared to conventional results, as indicated by the steeper slopes of the former; Choi et al. [9] predict the strongest variation of Nusselt number with Re. Also, the predictions for all cases from Peng et al. fall below those for a conventional channel.

In the turbulent regime (Fig. 6), the predictions of all investigators with the exception of Peng et al. [14] and Peng and Peterson [16] fall above the conventional channel values. In particular, Adams et al. 20] and Wu and Little [4] lie in one group. The predictions of Choi et al. [9] and Yu et al. [36] are also somewhat comparable, and lie in a different group. It may be noted that these groups are not divided by fluid type (since both groups include results for nitrogen and water) or by microchannel dimensions. The rectangular microchannels of different dimensions (Table 2) considered in Peng et al. [14] exhibit a large variation in predicted Nusselt numbers. In all these results, as well as for Peng and Peterson [16], the predicted values lie below those from the Dittus-Boelter correlation. Turbulent heat transfer predictions for case D are not included in this comparison since it appears that the value of $C_{h,t}$ for this case may have been erroneously listed in [14] as 0.0926, and instead, should have been 0.00926. This latter value would more closely match other values for $C_{h,t}$, and would also result in the predictions for case D lying in the same group as cases A, B and C.

CONCLUSION

A comparative study of the results of investigations in the literature on flow and heat transfer in microchannels has been compiled in tabular form, under various research topics. Correlations for single-phase friction factor and Nusselt number proposed by various investigators based on their experiments have been compared and contrasted with conventional correlations for larger, conventional tubes and channels in the laminar and turbulent flow regimes. A number of working fluid and substrate combinations, and shapes and configurations of the microchannels are included in this comparison. Little agreement is seen between the predictions of different investigators. The results are also not seen to be distinguished by fluid or substrate type or by microchannel dimensions and shapes.

The comparative study presented here points to differences between the flow and heat transfer in microchannels and that in channels of conventional sizes. However, the information in the literature thus far does not point to unequivocal trends of variation or reasons for such trends. There is no evidence that continuum assumptions are violated for the microchannels tested, most of which have hydraulic diameters of 50 μm or more. As such, analyses based on Navier-Stokes and energy equations would be expected to adequately model the phenomena observed, as long as the experimental conditions and measurements are correctly identified and simulated. The discrepancies in predictions may very well be due to entrance and exit effects, differences in surface roughness in the different microchannels investigated, nonuniformity of channel dimensions, nature of the thermal and flow boundary conditions, and uncertainties and errors in instrumentation, measurement and measurement locations. Given the diversity in the results in the literature, a reliable prediction of the heat transfer rates and pressure drops in microchannels is not currently possible for design applications such as microchannel heat sinks. There is a clear need for additional systematic studies which carefully consider each parameter influencing transport in microchannels.

Acknowledgement

REFERENCES

1. Tuckerman, D. B. and Pease, R. F. W., 1981, "High-performance heat sinking for VLSI," *IEEE Electron. Device Letters,* Vol. EDL-2, pp. 126-129.

2. Tuckerman, D. B. and Pease, R. F. W., 1982, "Ultrahigh thermal conductance microstructures for cooling integrated circuits," *Procs. 32nd Electronics Components Conf.,* IEEE, EIA, CHMT, pp. 145-149.

3. Wu, P. Y. and Little, W. A., 1983, "Measurement of friction factor for the flow of gases in very fine channels used for micro miniature Joule Thompson refrigerators," Cryogenics, Vol. 23, pp. 273-277.

4. Wu, P. Y. and Little, W. A., 1984, "Measurement of the heat transfer characteristics of gas flow in fine channel heat exchangers for micro miniature refrigerators," Cryogenics, Vol. 24, pp. 415-420.

5. Mahalingam, M. and Andrews, J., 1987, "High performance air cooling for microelectronics," *Procs. Int. Symp. on Cooling Technology for Electronic Equipment*, Honolulu, Hawaii, pp. 608-625.

6. Phillips, R. J., Glicksman, L. R., and Larson, R., 1987, "Forced convection, liquid-cooled, microchannel heat sinks for high-power-density microelectronics," *Procs. Int. Symp.Cooling Technology for Electronic Equip.,* Honolulu, HI, USA, pp. 227-248.

7. Pfahler, J., Harley, J., Bau, H. H., and Zemel, J., 1990, "Liquid transport in micron and submicron channels," *J. Sensors Actuators A*, Vol. 21-23, pp. 431-434.

8. Hoopman, T. L., 1990, "Microchanneled structures," *Microstructures, Sensors and Actuators*, ASME DSC-108, pp. 171-174.

9. Choi, S. B., Barron, R. F., and Warrington, R. O., 1991, "Fluid flow and heat transfer in microtubes," *Micromechanical Sensors, Actuators and Systems,* ASME DSC-Vol.32, pp. 123-134.

10. Rahman, M. M. and and Gui, F., "Experimental measurements of fluid flow and heat transfer in microchannel cooling passages in a chip substrate," *Advances in Electronic Packaging,* ASME EEP-Vol. 4-2, pp. 685-692.

11. Peng, X. F. and Wang, B. X., 1993, "Forced convection and flow boiling heat transfer for liquid flowing through microchannels," *Int. J. Heat Mass Transfer*, Vol. 14, pp. 3421-3427.

12. Wang, B. X. and Peng, X. F., 1994, "Experimental investigation on liquid forced convection heat transfer through microchannels," *Int. J. Heat Mass Transfer,* Vol. 37, Suppl. 1, pp.73-82.

13. Peng, X. F., Peterson, G. P., and Wang, B. X., 1994a, "Frictional flow characteristics of water flowing through microchannels", *Experimental Heat Transfer,* Vol. 7, pp. 249-264.

14. Peng, X. F., Peterson, G. P., and Wang, B. X., 1994b, "Heat transfer characteristics of water flowing through microchannels", *Experimental Heat Transfer,* Vol. 7, pp. 265-283.

15. Peng, X. F. and Peterson, G. P., 1995, "The effect of thermofluid and geometrical parameters on convection of liquids through rectangular microchannels," *Int. J. Heat Mass Transfer*, Vol. 38, pp. 755-758.

16. Peng, X. F. and Peterson, G. P., 1996a, "Convective heat transfer and flow friction for water flow in microchannel structures," *Int. J Heat Mass Transfer,* Vol. 39, pp. 2599-2608.

17. Peng, X. F. and Peterson, G. P., 1996b, "Forced convection heat transfer of single phase binary mixtures through microchannels," *Experimental Thermal and Fluid Science,* Vol. 12, pp. 98-104.

18. Harms, T.M., Kazmierczak, M., Gerner, F.M., Holke, A., Henderson, H.T., Pilchowski, J., and Baker, K., 1997, "Experimental investigation of heat transfer and pressure drop through deep microchannels in a (110) silicon substrate," ASME HTD-Vol.351-1, pp. 347-357.

19. Zhuang, Y., Ma, C. F., and Qin, M., 1997, "Experimental study on local heat transfer with liquid impingement flow in two-dimensional micro-channels," *Int. J. Heat Mass Transfer,* Vol. 40, pp. 4055-4059.

20. Adams, T. M., Abdel-Khalik, S. I., Jeter, S. M., and Qureshi, Z. H., 1998, "An experimental investigation of single-phase forced convection in microchannels," *Int. J Heat Mass Transfer,* Vol. 41, pp. 851-857.

21. Adams, T. M., Dowling, M. F., Abdel-Khalik, S. I., and Jeter, S. M., 1999, "Applicability of traditional turbulent single phase forced convection correlations to non-circular microchannels," *Int. J. Heat Mass Transfer,* Vol. 42, pp. 4411-4415.

22. Tso, C. P. and Mahulikar, S. P., 1998, "Use of the Brinkman number for single phase forced convective heat transfer in microchannels," *Int. J. Heat Mass Transfer*, Vol. 41, pp. 1759-1769.

23. Tso, C. P. and Mahulikar, S. P., 1999, "Role of the Brinkman number in analyzing flow transitions in microchannels," *Int. J. Heat Mass Transfer*, Vol. 42, pp. 1813-1833.

24. Tso, C. P. and Mahulikar, S. P., 2000, "Experimental verification of the role of Brinkman number in microchannels using local parameters," *Int. J. Heat Mass Transfer,* Vol. 43, pp. 1837-1849.

25. Ma, H. B., Peterson, G. P., and Lu, X. J., 1994, "Influence of vapor-liquid interactions on the liquid pressure drop in triangular microgrooves," *Int. J. Heat Mass Transfer*, Vol. 37, pp. 2211-2219.

26. Kleiner, M. B., Kuehn, S. A., and Haberger, K., 1995, "High performance forced air cooling scheme employing microchannel heat exchangers," *IEEE Trans. Components, Packaging and Manuf. Technol. A*, Vol. 18, pp. 795-804.

27. Takamatsu, K., Fujimoto, N., Rao, Y. F., and Fukuda, K., 1997, "Numerical study of flow and heat transfer of superfluid helium in capillary channels," *Cryogenics*, Vol. 37, pp. 829-835.

28. Copeland, D., Behnia, M., and Nakayama, W., 1997, "Manifold microchannel heat sinks: Isothermal analysis," *IEEE Transactions on Components, Packaging, and Manufacturing Technology – Part A,* Vol. 20, pp. 96-102.

29. Mala, G. M., Li, D., and Dale, J. D., 1997a, "Heat transfer and fluid flow in microchannels," *Int. J. Heat Mass Transfer*, Vol. 40, pp. 3079-3088.

30. Mala, G. M., Li, D., Werner, C., Jacobasch, H. J., and Ning, Y. B., 1997b, "Flow characteristics of water through a microchannel between two parallel plates with electrokinetic effects," *Int. J. Heat Fluid Flow*, Vol. 18, pp. 489-496.

31. Yang, C., Li, D., and Masliyah, J. H., 1998, "Modeling forced liquid convection in rectangular microchannels with electrokinetic effects," *Int. J. Heat Mass Transfer*, Vol. 41, pp. 4229-4249.

32. Bau, H. H., 1998, "Optimization of conduits' shape in microscale heat exchangers," *Int. J. Heat Mass Transfer*, Vol. 41, pp. 2717-2723.

33. Lee, D. Y. and Vafai, K., 1999, "Comparative analysis of jet impingement and microchannel cooling for high heat flux applications," *Int. J Heat Mass Transfer*, Vol. 42, pp. 1555-1568.

34. Arkilic, E. B., Breuer, K. S., and Schmidt, M. A., 1994, "Gaseous flow in microchannels," *Application of Microfabrication to Fluid Mechanics*, ASME FED-Vol. 197, pp. 57-66.

35. Arkilic, E. B., Schmidt, M. A., and Breuer, K. S., 1997, "Gaseous slip flow in long microchannels," *IEEE J. Microelectromechanical Systems*, Vol. 6, pp. 167-178.

36. Yu, D., Warrington, R., Barron, R., and Ameel, T., 1995, "An experimental and theoretical investigation of fluid flow and heat transfer in microtubes," *ASME/JSME Thermal Engineering Conference*, Vol. 1, pp. 523-530.

37. Mavriplis, C., Ahn, J. C., and Goulard., R., 1997, "Heat transfer and flow fields in short microchannels using direct simulation Monte Carlo," *AIAA J. Thermophysics and Heat Transfer*, Vol. 11, pp. 489-496.

38. Pfahler, J., Harley, J., Bau, H. H., and Zemel, J., 1991, "Gas and liquid flow in small channels," *Micromechanical Sensors, Actuators and Systems*, ASME DSC-32, pp. 49-60.

39. Kavehpour., H. P., Faghri, M., and Asako., Y., 1997, "Effects of compressibility and rarefaction on gaseous flows in microchannels," *Numerical Heat Transfer*, Vol. 32A, pp. 677-695.

40. Guo, Z. Y. and Wu, X.B., 1997, "Compressibility effect on the gas flow and heat transfer in a micro tube," *Int. J. Heat Mass Transfer*, Vol. 40, pp. 3251-3254.

41. Chen, C. S., Lee, S. M., and Sheu, J. D., 1998, "Numerical analysis of gas flow in microchannels," *Numerical Heat Transfer*, Vol. 33A, pp. 749-761.

42. Niu, Y. Y., 1999, "Navier-Stokes analysis of gaseous slip flow in long grooves," *Numerical Heat Transfer*, Vol. 36A, pp.75-93.

43. Bowers, M. B. and Mudawar, I., 1994a, "Two phase electronic cooling using mini-channel and micro-channel heat sinks. Part 1: Design criteria and heat diffusion constraints," *ASME J Electronic Packaging*, Vol. 116, pp. 290-297.

44. Bowers, M. B. and Mudawar, I., 1994b, "Two phase electronic cooling using mini-channel and micro-channel heat sinks. Part 2: Flow rate and pressure drop constraints," *ASME J Electronic Packaging*, Vol. 116, pp. 298-305.

45. Bowers, M. B. and Mudawar, I., 1994c, "High flux boiling in low flow rate, low pressure drop mini-channel and micro-channel heat sinks," *Int. J. Heat Mass Transfer*, Vol. 37, pp. 321-332.

46. Peng, X. F., Wang, B. X., Peterson, G. P., and Ma, H. B., 1995, "Experimental investigation of heat transfer in flat plates with rectangular microchannels," *Int. J. Heat and Mass Transfer,* Vol. 38, pp.127-137.

47. Peng, X. F., Peterson, G. P., and Wang, B.X., 1996, "Flow boiling of binary mixtures in microchannel plates," *Int. J. Heat Mass Transfer*, Vol. 39, pp. 1257-1264.

48. Peng, X. F., Hu, H. Y., and Wang, B. X., 1998, "Flow boiling through V-shape microchannels," *Experimental Heat Transfer*, Vol. 11, pp. 87-90.

49. Ha, J. M. and Peterson, G. P., 1996, "The Interline Heat Transfer of Evaporating Thin Films Along a Micro Grooved Surface," *ASME J. Heat Transfer*, Vol. 118, pp. 747-7545.

50. Ha, J. M. and Peterson, G. P., 1998, "Capillary performance of evaporating flow in microgrooves – An analytical approach for very small tilt angles," *ASME J. Heat Transfer*, Vol. 120, pp. 452-457.

51. Roach, G. M. Jr., Abdel-Khalik, S. I., Ghiaasiaan, S. M., Dowling, M. F., and Jeter, S. M., 1999, "Low-flow critical heat flux in heated microchannels," *Nuclear Science and Engineering*, Vol. 131, pp. 411-425.

52. Celata, G. P., Cumo, M., and Mariani, A., 1993, "Burnout in highly subcooled water flow boiling in small diameter tubes," *Int. J. Heat Mass Transfer*, Vol. 36, pp. 1269-1285.

53. Mertz., R., Wein, A., Groll, M., 1996, "Experimental investigation of flow boiling heat transfer in narrow channels," *Heat and Technology*, Vol. 14, pp. 47-54.

54. Sturgis, J. C. and Mudawar, I., 1999a, "Critical heat flux in a long, rectangular channel subjected to one-sided heating – I. Flow visualization," *Int. J. Heat Mass Transfer*, Vol. 42, pp. 1835-1847.

55. Sturgis, J. C. and Mudawar, I., 1999b, "Critical heat flux in a long, rectangular channel subjected to one-sided heating – II. Analysis of critical heat flux data," *Int. J. Heat Mass Transfer*, Vol. 42, pp. 1849-1862.

56. Cuta, J. M., McDonald, C. E., and Shekarriz, A., 1996, "Forced convection heat transfer in parallel channel array microchannel heat exchanger," *Advances in Energy Efficiency, Heat/Mass Transfer Enhancement*, ASME PID-Vol.2/HTD-Vol. 338, pp. 17-23.

57. Ravigururajan, T. S., 1998, "Impact of channel geometry on two phase flow heat transfer characteristics of refrigerants in microchannel heat exchangers," *ASME J. Heat Transfer*, V.120, pp. 485-491.

58. Triplett, K. A., Ghiaasiaan, S. M., Abdel-Khalik, S. I., and Sadowski, D. L., 1999a, "Gas-liquid two phase flow in microchannels. Part I: Two phase flow patterns," *Int. J. Multiphase Flow,* Vol. 25, pp. 377-394.

59. Triplett, K. A., Ghiaasiaan, S. M., Abdel-Khalik, S. I., LeMouel, A., and McCord, B. N., 1999b, "Gas-liquid two phase flow in microchannels. Part II: Void fraction and pressure drop," *Int. J. Multiphase Flow,* Vol. 25, pp. 395-410.

60. Coleman, J. W. and Garimella, S., 1999, "Characterization of two-phase flow patterns in small diameter round and rectangular tubes," *Int. J. Heat Mass Transfer*, Vol. 42, pp. 2869-2881.

61. Tuckerman, D. B., 1984, "Heat transfer microstructures for integrated circuits," Ph.D. Thesis, Stanford University, Stanford, California.

62. Weisberg, A., Bau, H. H., and Zemel, J., 1992, "Analysis of microchannels for integrated cooling," *Int. J. Heat Mass Transfer*, Vol. 35, pp. 2465-2474.

63. Roy, S. K. and Avanik, B. L., 1996, "Very high heat flux microchannel heat exchanger for cooling of semiconductor laser diode arrays," *IEEE Trans. Components, Packaging and Manuf. Technol. Part B: Advanced Packaging*, Vol. 19, pp. 444-451.

64. Aranyosi, A., Bolle, L. M. R., and Buyse, H. A., 1997, "Compact air-cooled heat sinks for power packages," *IEEE Trans. Components, Packaging and Manuf. Technol. Part A*, Vol. 20, pp. 442-451.

65. Perret, C., Schaeffer, C., and Boussey, J., 1998, "Microchannel integrated heat sinks in silicon technology," *IEEE Industry Applications Society Annual Meeting,* Vol. 2, 98CH36242, pp. 1051-1055.

66. Gillot, C., Schaeffer, C., and Bricard, A., 1998, "Integrated micro heat sink for power multichip module," *IEEE Industry Applications Society Annual Meeting,* Vol. 2, 98CH36242, pp. 1046-1050.

67. Gillot, C., Meysenc, L., and Schaeffer, C., 1999, "Integrated single and two phase micro heat sinks under IGBT chips," *IEEE Transactions on Components and Packaging Technology,* Vol. 22, pp. 384-389.

68. Yu, S., Ameel, T., and Xin, M., 1999, "An air-cooled microchannel heat sink with high heat flux and low pressure drop," *Procs. 33rd National Heat Transfer Conference,* Albuquerque, New Mexico, Paper No. NHTC 99-162, pp. 1-7.

69. Richter, M., Woias, P., and Weiβ, D., 1997, "Microchannels for applications in liquid dosing and flow-rate measurement," *Sensors and Actuators A,* Vol. 62, pp. 480-483.

70. Meinhart, C. D., Wereley, S. T., and Santiago, J. G., 1999, "PIV measurements of a microchannel flow," *Experiments in Fluids*, Vol. 27, pp. 414-419.

71. Gnielinski, V., 1976, "New equations for heat and mass transfer in turbulent pipe and channel flow," *International Chemical Engineering,* Vol. 16, pp. 359-368.

LIST OF FIGURE CAPTIONS

Fig. 1. Friction-factor predictions from the literature for microchannels and conventional channels, in the laminar and turbulent regimes.

Fig. 2. Friction-factor predictions in the laminar regime.

Fig. 3. Friction-factor predictions in the turbulent regime.

Fig. 4. Heat transfer predictions from the literature for microchannels and conventional channels, in the laminar and turbulent regimes.
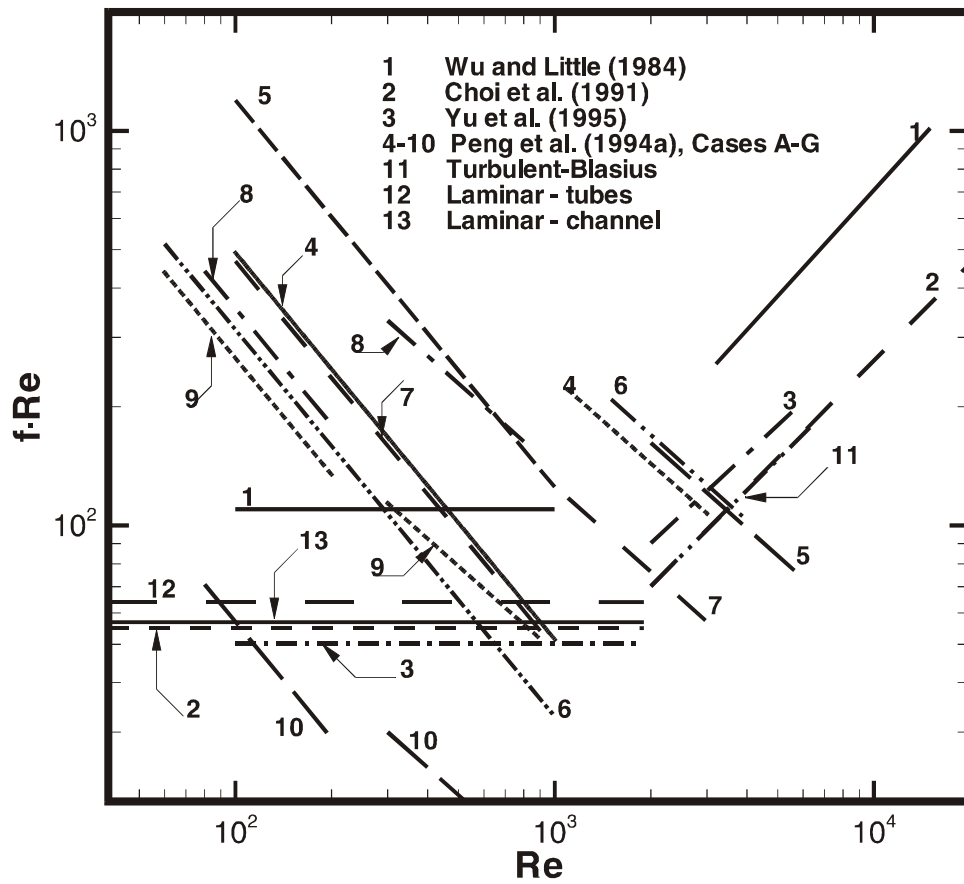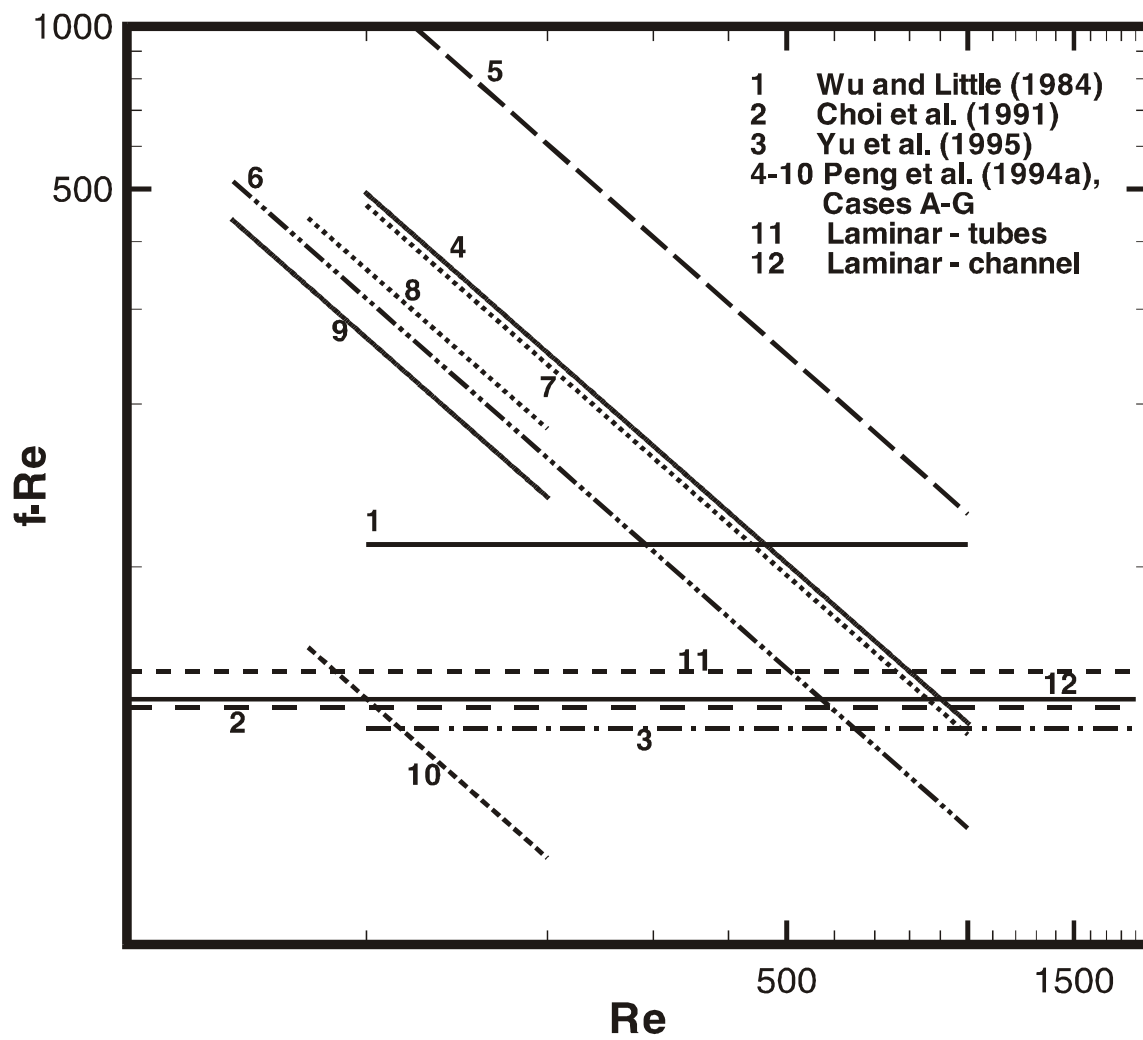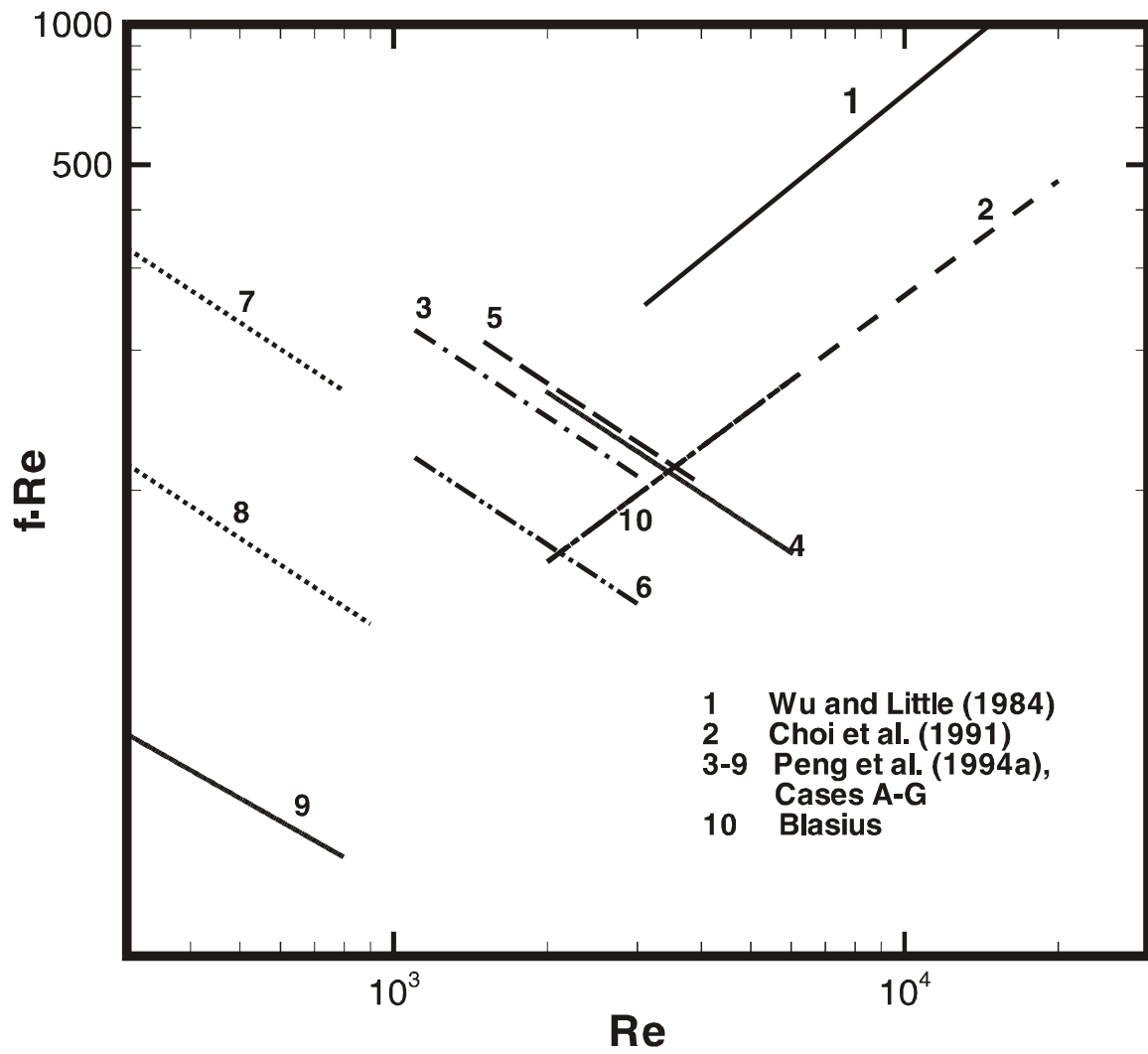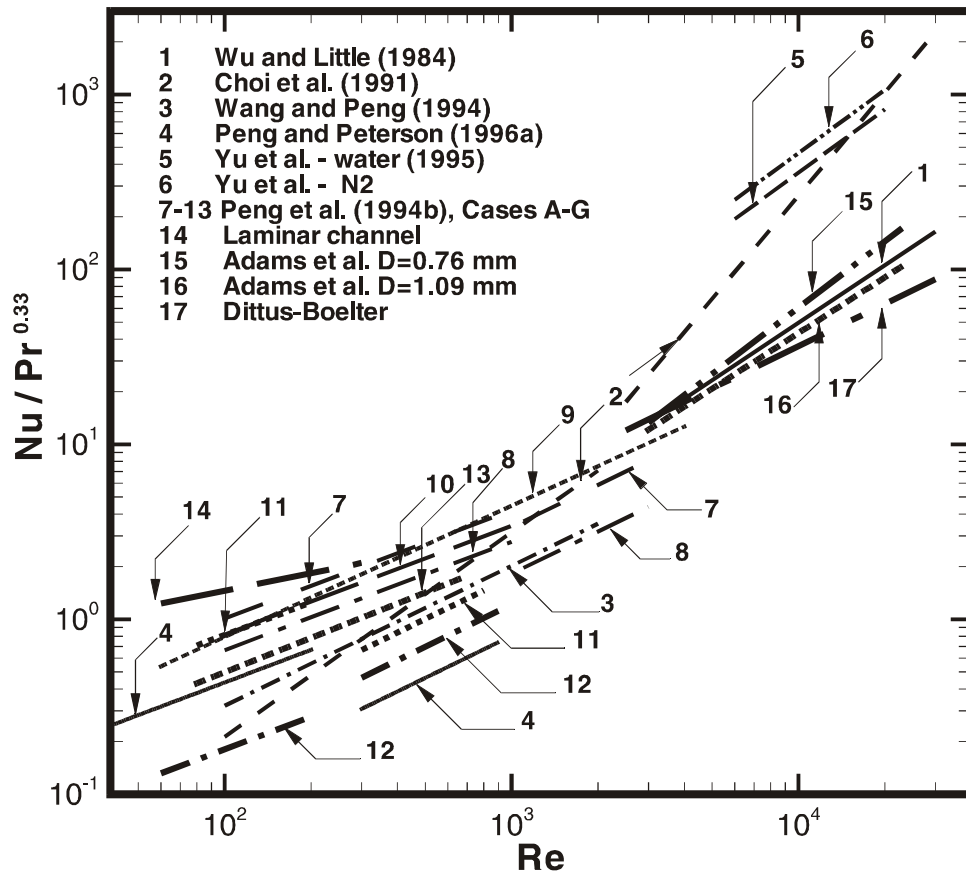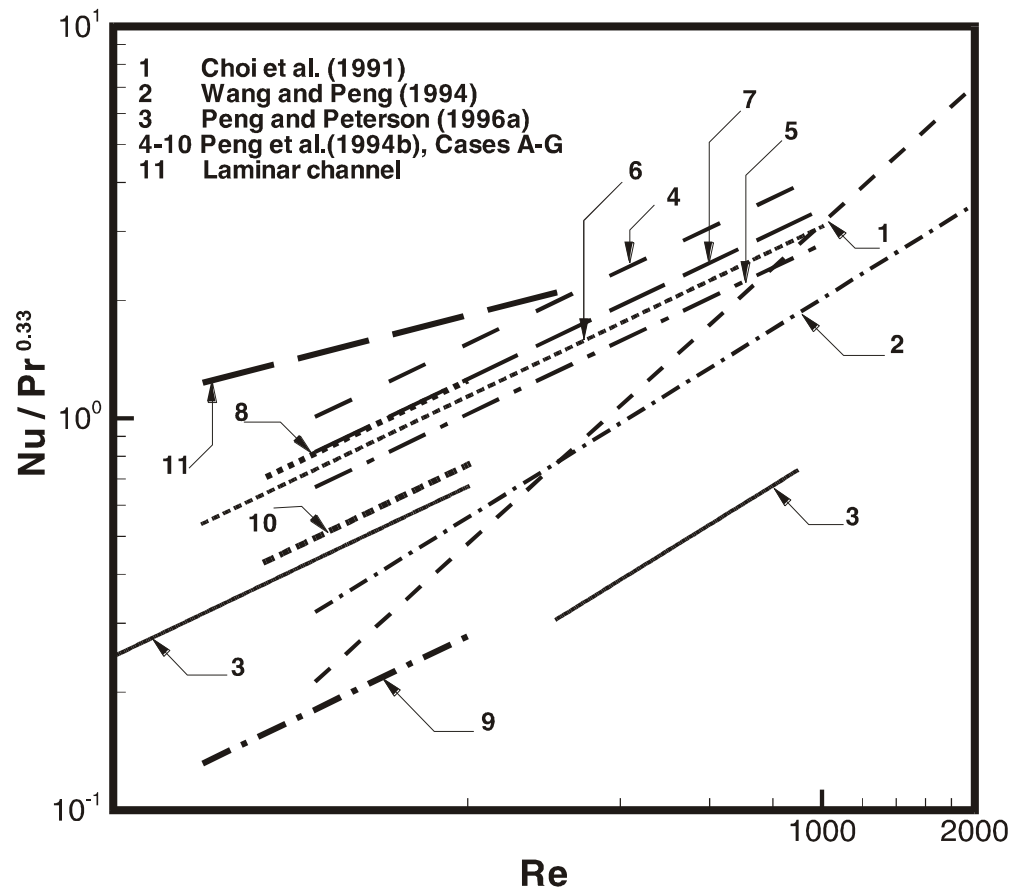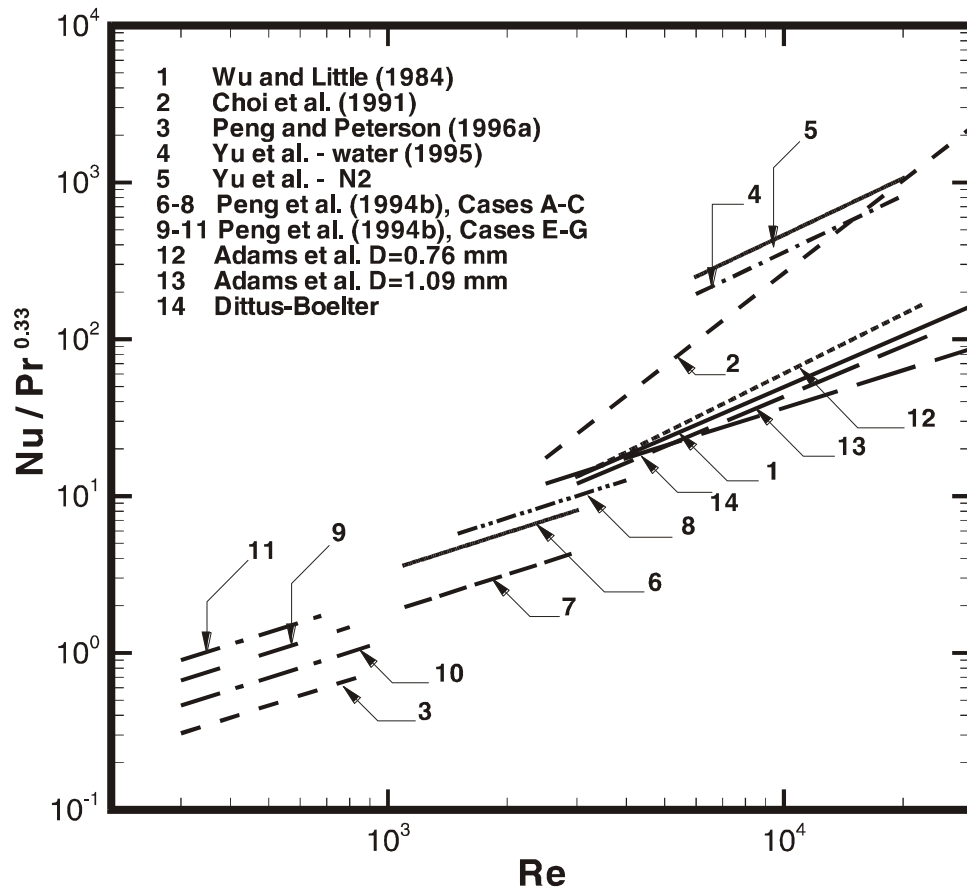
Fig. 5. Heat transfer predictions in the laminar regime.

Fig. 6. Heat transfer predictions in the turbulent regime.

LIST OF TABLE CAPTIONS

Table 1. Summary of Microchannel Studies in the Literature.

Table 2. Microchannel configurations and coefficients from Peng et al. [13, 14].

Fig. 1. Friction-factor predictions from the literature for microchannels and conventional channels, in the laminar and turbulent regimes.

Fig. 2. Friction-factor predictions in the laminar regime.

Fig. 3. Friction-factor predictions in the turbulent regime.

Fig. 4. Heat transfer predictions from the literature for microchannels and conventional channels, in the laminar and turbulent regimes.

Fig. 5. Heat transfer predictions in the laminar regime.

Fig. 6. Heat transfer predictions in the turbulent regime.

The plot shows Nu / Pr$^{0.33}$ versus Re on logarithmic axes, with the following legend:

1. Wu and Little (1984)
2. Choi et al. (1991)
3. Peng and Peterson (1996a)
4. Yu et al. - water (1995)
5. Yu et al. - N2
6-8 Peng et al. (1994b), Cases A-C
9-11 Peng et al. (1994b), Cases E-G
12. Adams et al. D=0.76 mm
13. Adams et al. D=1.09 mm
14. Dittus-Boelter

22

Configuration/Parameters	Nature of Work	Observations/Conclusions	Reference
MICROCHANNEL CONCEPTS AND EARLY WORK			
Rectangular cross section; water in silicon W = 50 μm; H = 300 μm Q = 4.7, 6.5, 8.6 cm^3/s	Experiments on integral heat sink for silicon integrated circuits	• Demonstrated use of microchannels for very high convective heat transfer in cooling integrated circuits (790 W/cm^2 at a substrate-to-coolant temperature difference of 71°C)	Tuckerman & Pease (1981) [1]
Microchannels in cooling of integrated circuits	Microchannel fabrication and implementation details discussed	• Coolant selection, packaging/headering, microstructure selection, fabrication and bonding discussed • Etching and precision-sawing compared; fabrication and advantages of 'micropillars' using precision-sawing discussed • Expressions for Coolant Figure of Merit provided: CFOM = $(k_c\rho C/\mu)^{0.25}$ for given coolant pressure, and $(k_c\rho^2 C^2/\mu)^{0.25}$ for given pumping power	Tuckerman & Pease (1982) [2]
Trapezoidal; nitrogen in silicon and glass W = 130-300 μm, H = 30-60 μm, D$_h$ = 55-76 μm	Friction factors measured and compared with Moody's chart values for commercial channels	• Friction factor for glass channels 3-5 times larger than smooth-pipe predictions • Flow transition occurred at Re $\approx$ 400 • Correlations for friction factor $f = (110\pm8) / Re$ Re $\leq$ 900 $f = 0.165 (3.48 - \log Re)^{2.4} + (0.081\pm 0.007)$ 900 < Re < 3000 $f = (0.195 \pm 0.017) / Re^{0.11}$ 3000 < Re < 15000	Wu & Little (1983) [3]
As in [3]	Heat transfer experiments	• Correlation for Nusselt number in the turbulent regime: $Nu = 0.0022\, Pr^{0.4}\, Re^{1.09}$ Re > 3000	Wu & Little (1984) [4]
Rectangular; air in silicon W = 0.13-0.25 mm, H/W = 10, A$_s$ = 47-63 cm^2/cm^3	Comparison of performance with conventional heat sinks, based on correlations	• Micro-structured compact heat sinks attractive compared to conventional air circulation heat sinks	Mahalingam & Andrews (1987) [5]
Rectangular; water in silicon W = 50-600μm	Theoretical model for fully developed, developing flows	• Turbulent flow designs showed equivalent or better performance compared to laminar flow designs	Phillips et al. (1989) [6]
Rectangular; N Propanol in silicon A$_c$ = 80-7200 sq. μm	Experiments	• Channels with larger cross-sectional areas showed better agreement with theoretical predictions for the friction factor • Proposed f = C/Re with C given as C vs. Re graphs (laminar)	Pfahler et al. (1990) [7]
Microchannel structures for cooling applications	Microchannel applications discussed	• Applications of microchannels to electronics cooling, compact heat exchangers, heat shields and fluid distribution systems discussed	Hoopman (1990) [8]

Configuration/Parameters	Nature of Work	Observations/Conclusions	Reference

Microtubes; nitrogen in silica
D = 3, 7, 10, 53, 81 μm, L = 24-52 mm
	Experiments on friction and heat transfer	• Correlations for friction factor and Nusselt number:
		  Laminar (Re < 2000) $f = 64/Re\,[1+30(v/Dc_a)]^{-1}$
		  Turbulent (2500 < Re < 20000) $f = 0.140\,Re^{-0.182}$
		  Laminar $Nu = 0.000972\,Re^{1.17}\,Pr^{1/3}$
		  Turbulent $Nu = 3.82 \times 10^{-6}\,Re^{1.96}\,Pr^{1/3}$
			Choi et al. (1991) [9]

Rectangular; water in etched silicon W = 1 mm, H = 176-325 μm, L = 46 mm, P = 2 mm	Experiments	• Nusselt numbers higher than those predicted from analytical solutions for developing laminar flow	Rahman & Gui (1993) [10]
SINGLE-PHASE (LIQUID) EXPERIMENTS			
Rectangular; deionized water in stainless steel W = 0.6 mm; H = 0.7 mm, T_i = 30-60°C, v = 0.2-2.1 m/s	Experiments on single-phase forced convection	• In single-phase convection, a steep increase in wall heat flux with the wall temperature • Heat flux for microchannels higher than for normal-size tube	Peng & Wang (1993) [11]
Rectangular; water, methanol in stainless steel W = 0.2, 0.4, 0.6, 0.8 mm, H = 0.7 mm, T_i = 10-35°C (water), 14-19°C (methanol), v = 0.2-2.1 m/s	Experiments on forced convection flow and heat transfer	• Heat transfer augmented as liquid temperature was reduced and as liquid velocity was increased • Fully developed turbulent convection regime starts at Re = 1000-1500 • Correlation for turbulent heat transfer $Nu = 0.00805\,Re^{4/5}\,Pr^{1/3}$	Wang & Peng (1994) [12]

Rectangular; water in stainless steel
D_h = 0.133-0.367 mm, L = 50 mm, H/W = 0.333-1, T_i = 22-44°C, v = 0.25-12 m/s, Re = 50-4000
	Experiments on frictional behavior in laminar and turbulent flow	• Flow transition occurred for Re = 200-700
		• Correlations proposed (values for $C_{f,l}$, $C_{f,t}$ provided in Table 2)
		  $f = C_{f,l}/Re^{1.98}$ laminar flow
		  $f = C_{f,t}/Re^{1.72}$ turbulent flow
			Peng et al. (1994a) [13]

As in [13]	Experiments on forced convection heat transfer characteristics	• Fully turbulent convective conditions reached at Re = 400-1500
		• Transition Re diminished with a reduction in microchannel dimension
		  $Nu = C_{h,l}\,Re^{0.62}\,Pr^{1/3}$ Laminar
		  $Nu = C_{h,t}\,Re^{0.8}\,Pr^{1/3}$ Turbulent
		  (values for $C_{h,l}$, $C_{h,t}$ provided in Table 2)
			Peng et al. (1994b) [14]

As in [12] except T_i = 11-28°C (water), 12-20°C (methanol) v = 0.2-2.1 m/s (water), 0.2-1.5 m/s (methanol)	Experiments on effect of thermofluid properties and geometry on convective heat transfer	• Changes in flow regimes and heat transfer modes initiated at lower Re in microchannels compared to conventional channels • Transition zone and heat transfer characteristics in laminar and transition flow influenced by liquid temperature, velocity, Re and microchannel size	Peng & Peterson (1995) [15]
As in [13]	Experiments on single-phase flow and heat transfer	• Ratio of experimental to theoretical friction factor at critical Re plotted as a function of Z (= min [H,W] / max [H,W]) • Correlations proposed $Nu = 0.1165\,(D_h/P)^{0.81}(H/W)^{-0.79}\,Re^{0.62}\,Pr^{0.33}$ Laminar $Nu = 0.072\,(D_h/P)^{1.15}\,[1 - 2.421\,(Z-0.5)^2]\,Re^{0.8}\,Pr^{0.33}$ Turbulent	Peng & Peterson (1996a) [16]

Configuration/Parameters	Nature of Work	Observations/Conclusions	Reference
Rectangular; water-methanol mixture in stainless steel D_h = 0.133-0.367 mm, L = 50 mm W = 0.1, 0.2, 0.3, 0.4 mm, H = 0.2, 0.3 mm, T_i = 14-36°C, v = 0.04-3.8m/s, Re = 6-3500	Experiments	• Laminar heat transfer ceased for Re ≈ 70-400 depending on flow conditions; fully developed turbulent heat transfer achieved at Re = 200-700, depending on D_h • Transition Re reduced with a reduction in microchannel size • D_h, H/W and mixture mole fraction influenced heat transfer • Heat transfer increased for smaller mole fractions of the more volatile component	Peng & Peterson (1996b) [17]
Rectangular; deionized water in silicon W = 251 μm, H = 1030 μm, D_h = 404 μm, L = 2.5 cm, Q = 5.47-118 cm^3/s	Experimental & theoretical study	• Critical Re of 1500 identified for onset of turbulence • Analysis showed that flow and heat transfer performance could be improved by increasing H, and that for the same pressure drop and pumping power, thermal resistance was smaller for deeper channels	Harms et al. (1997) [18]
Rectangular; FC-72 and transformer oil in stainless steel H = 0.10-0.58 mm; nozzle dimensions (mm): Length = 35, B = 0.146, 0.210, 0.234, Height = 12, v = 0.54-8.45 m/s Re = 70-170 (oil), 911-4807 (FC72)	Experiments in impingement on 2D microchannels	• Empirical correlation for Nusselt number for the two liquids Nu_x = 0.429 Re$^{0.583}$ Pr$^{1/3}$ (x / 2H)$^{0.349}$ (B/2H)$^{-0.494}$	Zhuang et al. (1997) [19]
Circular; distilled water in copper D = 0.102-1.09 mm v < 18.9 m/s, Re = 2.6 x 10^3 – 2.3 x 10^4, Pr = 1.53-6.43 q" < 3.0 MW/m^2	Experiments on turbulent single-phase flow	• Nusselt numbers higher than those predicted by large-channel correlations • Gnielinski [71] correlation modified for Nusselt number for turbulent flow in circular microchannels (f from Filonenko, 1954): $Nu = Nu_{Gn} (1+F)$ where $F = C$ Re $[1-(D/D_o)^2]$ $Nu_{Gn} = (f/8)(Re - 1000)Pr / [1+12.7(f/8)^{1/2}(Pr^{2/3}-1)]$ $C = 7.6 \times 10^{-5}$; D_o = 1.164 mm, f = [1.82 log (Re) – 1.64]$^{-2}$	Adams et al. (1998) [20]
Non-circular; water in copper D_h = 1.13 mm, Re = 3.9x10^3 - 2.14x10^4, Pr = 1.22-3.02	Experiments on turbulent convection	• Experimental Nusselt number well-predicted by Nu $_{Gn}$ • D_h ≈ 1.2 mm proposed as reasonable lower limit for applicability of standard Nusselt-type correlations to non-circular channels	Adams et al. (1999) [21]
Rectangular laminar and transition flow	Dimensional analysis based on experimental data in the literature	• Attempted to explain the observation that Nu may decrease with increasing Re in laminar regime and may remain unaffected in transition regime • Proposed that Brinkman number may better correlate convective heat transfer	Tso & Mahulikar (1998, 1999) [22, 23]
Almost circular; water in aluminum D_h = 0.73 mm	Experiments	• Laminar flow data found to correlate well using Brinkman number	Tso & Mahulikar (2000) [24]
SINGLE-PHASE (LIQUID) MODELS AND OPTIMIZATION STUDIES			
Triangular microgrooves channel angle 20-60 deg.	Analytical/numerical analysis	• Friction factor-Reynolds number product strongly dependent on channel angle, contact angle, and dimensionless vapor-liquid interface flow number	Ma et al. (1994) [25]

Configuration/Parameters	Nature of Work	Observations/Conclusions	Reference
Microchannel plate-fin heat sink; air in copper, aluminum W = 400, 500 μm, H = 2.5 cm, Q = 1-6 l/s	Thermal resistance model, experiments, optimization	• Thermal resistance of microchanneled heat sink lower than for heat sinks employing direct air cooling, by a factor of more than 3	Kleiner et al. (1995) [26]
Circular capillary channels D = 8.1-96 μm, 0.76-4.7 μm	Numerical study on the flow of superfluid Helium using a "two-fluid model"	• Existence of an optimum channel diameter for maximum mass flow rate indicated	Takamatsu et al. (1997) [27]
Rectangular; fluorocarbon in silicon P = 100-1000 μm, H = 150-200 μm, W = 56.6-113.4 μm, v = 0.1-1.0 m/s	Numerical analysis of manifold microchannel heat sinks	• 3D model showed close agreement with simple 1D model at high inlet velocity • Numerical results showed much weaker effect of W compared to analytical results • L had almost no effect on thermal resistance and affected only pressure drop	Copeland et al. (1997) [28]
Parallel plates at 25 μm separation dilute aqueous electrolyte L = 10 mm	Theoretical analysis incorporating effects of electric double layer field	• EDL resulted in a reduced flow velocity than in conventional theory, thus affecting temperature distribution and reducing Re • Higher heat transfer predicted without the double layer	Mala et al. (1997a) [29]
Parallel plates (10 x 20 mm) of P-type silicon and glass at 10-280 μm separation; ΔP = 0-350 mbar	Experimental study and comparison with predicted volume flow rates	• For solutions of high ionic concentration as well as for D_h > few hundred μm, EDL effect negligible • EDL effect becomes significant for dilute solutions	Mala et al. (1997b) [30]
Rectangular; dilute aqueous electrolyte in silicon H = 20 μm, W = 30 μm, L = 10 mm, ΔP = 2 atm, T_i = 298 K, q'' = 1.0 x 10^5 W/m^2	Numerical analysis with effects of EDL and flow-induced electrokinetic field	• The EDL field and electrokinetic potential act against the liquid flow, resulting in higher friction coefficient, reduced flow rate and a reduced Nusselt number, for dilute solutions	Yang et al. (1998) [31]
Rectangular (flat plate micro heat exchangers)	Optimization study on microchannel shape	• Width of heat exchanger conduits may be optimized to reduce maximum temperature of the uniformly heated surface	Bau (1998) [32]
Microchannel cooling and jet impingement	Comparative analysis of jet impingement and microchannel cooling	• Thermal performance of jet impingement without any treatment of spent flow substantially lower than microchannel cooling, regardless of target dimension • Microchannel cooling preferable for target dimensions smaller than 7x7 cm	Lee and Vafai (1999) [33]
GAS FLOW			
Rectangular; helium in silicon W = 52.25 μm, H = 1.33 μm, L = 7500 μm; Inlet to outlet pressure ratio = 1.2-2.5, Re = (0.5-4)x10^{-3}	Flow rates measured and compared with theoretical model	• Mass flow–pressure relationship accurately modeled by including a slip flow boundary condition at the wall	Arkilic et al. (1994) [34]
As in [34] with pressure ratio = 1.6-4.2, Re = (1.4-12) x10^{-3}	Experiments and comparison of mass flow with results from 2D analysis with slip boundary condition	• Discussions on nondimensional formulation and perturbation solution	Arkilic et al. (1997) [35]

Configuration/Parameters	Nature of Work	Observations/Conclusions	Reference

Microtubes; nitrogen and water in silica D = 19, 52, 102 μm, Pr = 0.7-5, Re = 250-20000	Experiments; theoretical scaling analysis	• Turbulent momentum and energy transport in the radial direction significant in the near-wall zone of a microtube
		• Correlations proposed:
		  $f = 50.13/Re$ (laminar, Re < 2000)
		  $f = 0.302/Re^{0.25}$ (transition, 2000 < Re < 6000)
		  $Nu = 0.007Re^{1.2}\,Pr^{0.2}$ (turbulent, 6000 < Re < 20000)
			Yu et al. (1995) [36]

Rectangular H = 0.5, 5 μm, H/W = 2.5, 5, 10, 20 (subsonic); 5, 10, 20 (supersonic)	Numerical study using direct simulation Monte Carlo technique	• Heat flux on the channel surface decreases with increase in Knudsen number and channel length in supersonic flow	Mavriplis et al. (1995) [37]
Rectangular helium (as in [34]) helium and nitrogen, D_h = 1.01μm , L = 10.9 mm (as in [38])	2D numerical model, comparison with experiments in literature	• Nusselt number and friction coefficient substantially reduced for slip flows compared to continuum flows • Effect of compressibility significant at high Re	Kavehpour & Faghri (1997) [39]
Smooth microtubes Gas flow	Numerical solution of gas flow in microtubes	• Local Nusselt number increased with dimensionless length, due to compressibility • f-Re product not constant; dependent on Re	Guo & Wu (1997) [40]
Rectangular; nitrogen, helium in silicon W = 40 μm, H = 1.2 μm, L = 3 mm (N_2), W = 52 μm, H = 1.33 μm, L = 7.5 mm (He)	Numerical solution with slip boundary condition	• Small velocities and high pressure gradients due to large wall shear stresses • Comparisons with experiments of [34]	Chen et al. (1998) [41]
3D straight and spiral grooves	Numerical study on slip flow in long microchannels	• Non-linear pressure gradients along the microchannels due to density variations	Niu (1999) [42]
BOILING IN MICROCHANNELS			
Circular; R-113 in copper D = 2.45 mm (mini), 510 μm (micro) Q = 19-95 ml/min, ΔT: 10-32°C	Experiments on boiling & two-ϕ flow; boiling curves & CHF values obtained	• Microchannel yielded higher CHF (28% greater at Q = 64 ml/min) than mini channel, with a larger ΔP (0.3 bar for micro, 0.03 bar for mini)	Bowers & Mudawar (1994a) [43]
As in [43]	Pressure drop model developed; predictions compared to experiments	• Major contributor to pressure drop identified as the acceleration resulting from evaporation • Compressibility effect important for microchannel when Mach number > 0.22 • Channel erosion effects more predominant in microchannels than in mini channels	Bowers & Mudawar (1994b) [44]
As in [43]	Experiments on boiling and two-phase flow	• Single CHF correlation for mini and microchannels developed: $q_{m,p}/(G\,h_{fg}) = 0.16\ We^{-0.19}\left(L/D\right)^{0.54}$	Bowers & Mudawar (1994c) [45]

Configuration/Parameters	Nature of Work	Observations/Conclusions	Reference
Rectangular; water in stainless steel $W = 0.6$ mm, $H = 0.7$ mm, $T_i = 30\text{-}60°C$, $v = 1.5 - 4.0$ m/s	Experiments on subcooled boiling of water	• Nucleate boiling intensified and wall superheat for flow boiling smaller in microchannels than in normal-sized channels for the same wall heat flux • No partial nucleate boiling observed in microchannels	Peng & Wang (1993) [11]
Rectangular; methanol in stainless steel $W = 0.2, 0.4, 0.6$ mm, $H = 0.7$ mm, $L = 45$ mm, $P = 2.4\text{-}4$ mm; $T_i = 14\text{-}19°C$ (Subcooling: 45-50°C), $v = 0.2\text{-}1.5$ m/s	Experiments on boiling	• Liquid velocity and subcooling do not affect fully developed nucleate boiling • Greater subcooling increased velocity and suppressed initiation of flow boiling	Peng et al. (1995) [46]
Rectangular; methanol-water mixture in stainless steel $W = 0.1, 0.2, 0.3, 0.4$ mm, $H = 0.2, 0.3$ mm, $L = 45$ mm, $D_h = 0.133\text{-}0.343$ mm, $v = 0.1\text{-}4.0$ m/s, $T_i = 18\text{-}27.5°C$ (Subcooling: 38-82°C)	Experiments on flow boiling in binary mixtures	• Heat transfer coefficient at onset of flow boiling and in partial nucleate boiling greatly influenced by concentration, microchannel/substrate dimensions, flow velocity and subcooling • These parameters had no significant effect on heat transfer coefficient in the fully nucleate boiling regime • Mixtures with small concentrations of methanol augmented flow boiling heat transfer	Peng et al. (1996) [47]
V-shaped; water and methanol in stainless steel Groove angle: 30-60 deg; $D_h = 0.2\text{-}0.6$ mm v (water) $= 0.31\text{-}1.03$ m/s v (methanol) $= 0.12\text{-}2.14$ m/s	Experiments on flow boiling	• Heat transfer and pressure drop were affected by flow velocity, subcooling, D_h and groove angle • No bubbles observed in microchannels during flow boiling, unlike in conventional channels • Experiments indicated an optimum D_h and groove angle	Peng et al. (1998) [48]
V-shaped	Analysis of microgrooves with non-uniform heat input	• Analytical expression developed for the evaporating film profile	Ha & Peterson (1996) [49]
V-shaped	Analysis of axial flow of evaporating thin film	• Used perturbation method to solve the axial flow of an evaporating thin film through a V-shaped microchannel with tilt	Ha & Peterson (1998) [50]
Circular and rod bundle; water in copper $D = 1.17, 1.45$ mm, $D_h = 1.131$ mm $m = 250\text{-}1000$ kg/m^{2}s Exit pressure $= 344\text{-}1043$ kPa Inlet pressure $= 407\text{-}1204$ kPa $T_i = 49\text{-}72.5°C$	Experiments on CHF in flow of subcooled water	• CHF found to increase monotonically with increasing mass flux or pressure • CHF depends on the channel cross section geometry, and increases with increasing D	Roach et al. (1999) [51]
BOILING IN SMALL DIAMETER TUBES AND CHANNELS			
Circular; water in stainless steel $D = 2.5$ mm, $t = 0.25$ mm, $v = 10\text{-}40$ m/s	Experiments on subcooled flow boiling of water under high heat fluxes	• Experimental data did not match predictions from CHF correlations in the literature	Celata et al. (1993) [52]
Rectangular; water and R141b in copper $W = 1, 2, 3$ mm, $H/W < 3$, $m = 50, 200, 300$ kg/m^{2}s	Experiments on flow boiling in narrow channels of planar heat exchanger elements	• Boiling curves and variations of heat transfer coefficient with local and average heat fluxes obtained	Mertz et al. (1996) [53]

Configuration/Parameters	Nature of Work	Observations/Conclusions	Reference
Rectangular; FC-72 in fiberglass W = 5 mm, H = 2.5 mm, Heated length = 101.6 mm, v = 0.25-10 m/s, Re = 2000-130000 Subcooling at outlet = 3, 16, 29°C	CHF experiments on long channels; flow visualization	• Propagation of vapor patches resembling a wavy vapor layer along the heated wall at the critical heat flux • Length and height of vapor patch found to increase along flow direction, and decreased with increasing subcooling and velocity	Sturgis & Mudawar (1999a) [54]
As in [54]	Theoretical model for CHF; data analysis	• Effect of periodic distribution of vapor patches idealized as a sinusoidal interface with amplitude and wavelength increasing in flow direction	Sturgis & Mudawar (1999b) [55]
TWO-PHASE FLOW			
Rectangular; R124 in copper W = 0.27 mm, H = 1.0 mm, D_h = 425 mm, Re_{Dh} = 100-750; q'' < 40 W/cm^2	Experiments on microchannel heat exchanger	• Nusselt number (~ 5 to 12) showed an increase with Reynolds number in single-ϕ flow, but was approximately constant in two-ϕ flow	Cuta et al. (1996) [56]
Rectangular; R124 in copper W = 270 μm, H = 1000 μm, L = 2.052 cm, D_h = 425 μm; Inlet subcooling: 5-15°C; Q = 35-300 ml/min	Experiments with two microchannel patterns (parallel and diamond)	• Heat transfer coefficient and pressure drop found to be functions of flow quality and mass flux, in addition to the heat flux and surface superheat • Heat transfer coefficient decreased by 20-30% for an increase in exit vapor quality from 0.01 to 0.65	Ravigururajan (1998) [57]
Circular and semi-triangular; air-water mixture in glass D = 1.1, 1.45 mm, D_h = 1.09, 1.49 mm, v(air): 0.02-80 m/s, v(water): 0.02-8 m/s (superficial velocity)	Visual observation of flow patterns and pattern maps	• Bubbly, churn, slug, slug-annular and annular flow patterns observed	Triplett et al. (1999a) [58]
As in [58]	Frictional pressure drops measured and compared with various two-ϕ friction models	• Models and correlations overpredicted channel void fraction and pressure drop in annular flow pattern • Annular flow interface momentum transfer and wall friction in microchannels significantly different from those in larger channels	Triplett et al (1999b) [59]
Circular and rectangular; air-water mixture in glass D_h = 1.3-5.5 mm; v = 0.1-100 m/s (gas); v = 0.01-10 m/s (liquid)	Experiments, flow visualization	• Tube diameter influences the superficial gas and liquid velocities at which flow transitions take place, due to combined effect of surface tension, hydraulic diameter and aspect ratio	Coleman & Garimella (1999) [60]
DESIGN AND TESTING			
Rectangular; water in silicon	Numerical solution for temperature field; comparison with experiments [61]	• Design algorithm developed for selection of heat exchanger dimensions • Expression for maximum pumping power obtained as function of channel geometry	Weisberg et al. (1992) [62]

Configuration/Parameters	Nature of Work	Observations/Conclusions	Reference
Almost rectangular; water in copper 0.5 x 12 mm, 0.125 x 12 mm Q = 0.47-5 gpm	Design and testing, microchannel heat exchanger for laser diode arrays	• Thermal resistance due to solder bond estimated	Roy & Avanic (1996) [63]
Rectangular and almost triangular; air in copper, aluminum	Parametric studies and experiments of air impingement in microchannels	• Thermal resistance model developed • Parametric studies to determine influence of static pressure, pumping power and geometric parameters on thermal resistance	Aranyosi et al (1997) [64]
Rectangular, diamond-shaped and hexagonal; water in silicon	3D numerical model; optimization for reducing thermal resistance	• Rectangular geometry had the lowest thermal resistance	Perret et al. (1998) [65]
Rectangular; water, FC72 in copper	Experiments on micro heat sink for power multichip module; 3D and 1D thermal resistance models	• Power densities of 230-350 W/cm^2 dissipated with a temperature rise of 35°C, and a pumping power of about 1W per chip • Parameter 'heat spread effect' defined $s = (R_{th1D} - R_{th3D}) / R_{th1D}$	Gillot et al. (1998) [66]
Rectangular; water, FC72 in copper W = 230, 311 μm, H = 730, 3040 μm, Q (ml/min) = 1350 (water, 1-ϕ) and 30 (2-ϕ); 2000 (FC 72 1-ϕ) and 300 (2-ϕ)	Experiments on single and two-phase micro heat exchangers for cooling transistors	• Two-phase heat exchanger provided lower thermal resistance and pressure drop compared to single-phase heat exchangers	Gillot et al. (1999) [67]
Rectangular; air in copper W = 800 μm, H = 50 mm, Q = 140 m^3/hr	Experiments and thermal resistance model	• Pressure drop found to have large deviation from predicted values at high air flow rates • Cooling capacity $\approx$ 1700 W at heat flux $\approx$ 15 W/cm^2	Yu et al. (1999) [68]
MEASUREMENT TECHNIQUES			
Triangular; water in silicon W = 28-182 μm, Q = 0.01-1000 μl/min	Optical flow measurements using microscope	• Measured flow rates in good agreement with theoretical values for laminar flow through triangular channels	Richter et al. (1997) [69]
Rectangular; water in glass W = 300 , H = 30, L = 25 mm	Particle image velocimetry	• Results agreed well with analytical solutions for Newtonian flow in rectangular channels	Meinhart et al. (1999) [70]

NOMENCLATURE

A_c	cross sectional area	k_c	coolant thermal conductivity	$R_{th\ 3D}$	thermal resistance from 3D analysis
A_s	surface area	L	length	Re	Reynolds number
B	slot width	Nu	Nusselt number	T_i	inlet temperature
C	coolant heat capacity	Nu_{Gn}	Nusselt number (Gnielinski correlation)	t	tube wall thickness
c_a	acoustic velocity			v	inlet velocity
D	diameter	P	channel pitch	W	width of microchannel
D_h	hydraulic diameter	Pr	Prandtl number	We	Weber number
f	friction factor	ΔP	pressure drop	x	distance from stagnation point
G	mass velocity ($\equiv$ m, mass flux)	Q	volumetric flow rate	ρ	density
H	height (depth) of microchannel	$q_{m,p}$	CHF based on heated channel area	μ	dynamic viscosity
h_{fg}	latent heat of vaporizaton	$R_{th\ 1D}$	thermal resistance from 1D analysis	ν	kinematic viscosity

Table 2. Microchannel configurations and coefficients from Peng et al. [13, 14].

Case	W, mm	H, mm	L, mm	D_h, mm	H/W	Re_{cr}	$C_{f, l}$	$C_{f, t}$	$C_{h, l}$	$C_{h, t}$
A	0.4	0.3	50	0.343	0.75	700	44800	34200	0.058	0.0134
B	0.3	0.3	50	0.3	0.1	700	109000	38600	0.0384	0.00726
C	0.4	0.2	50	0.267	0.5	700	28600	40400	0.0426	0.0166
D	0.3	0.2	50	0.24	0.667	400	42600	18200	0.0472	∗
E	0.2	0.2	50	0.2	1	200	32400	20100	0.0468	0.00696
F	0.3	0.1	50	0.15	0.333	200	24200	6920	0.0104	0.00483
G	0.2	0.1	50	0.133	0.5	200	5200	1820	0.0285	0.00939